OncoTargets and Therapy

Dovepress
Taylor & Francis Group

Open Access Full Text Article

ORIGINAL RESEARCH

NG25 Enhances Anti-Tumor Immunity in *KRAS*-Mutant Colorectal Cancer

Qi Xiang[1,*], Zhigang Mao[2,*], Qizhao Ma[1], Mi Su[1], Deng Tang[1], Siqi Lan[1], Yufei Tang[1], Ji Zhang[1], Yufang Wang[1]

[1]West China School of Basic Medical Sciences & Forensic Medicine, Sichuan University, Chengdu, Sichuan, People's Republic of China; [2]Department of Laboratory Medicine, West China Hospital, Sichuan University, Chengdu, Sichuan, People's Republic of China

*These authors contributed equally to this work

Correspondence: Ji Zhang; Yufang Wang, West China School of Basic Medical Sciences & Forensic Medicine, Sichuan University, No. 17 Renmin South Road, Chengdu, Sichuan, 610041, People's Republic of China, Email zhangj@scu.edu.cn; wangyufang@scu.edu.cn

Purpose: The poor prognosis of *KRAS*-mutant colorectal cancer is attributed to its immunosuppressive tumor microenvironment and the lack of effective targeted therapies. Transforming growth factor-β-activated kinase 1 (TAK1), serving as a critical upstream regulator of both the NF-κB and MAPK signaling pathways, promotes tumor progression through its aberrant activation. In this study, we aimed to investigate the anti-tumor and immunomodulatory effects of the TAK1 inhibitor NG25 in *KRAS*-mutant colorectal cancer, focusing on its impact on T cell differentiation, PD-L1 expression, and tumor immune microenvironment remodeling.

Methods: The anti-tumor and immune-enhancing effects of NG25 were evaluated through an in vitro tumor cell-lymphocyte co-culture system, and the orthotopic colorectal cancer models in both immunodeficient Balb/c nude mice and immunocompetent Balb/c mice.

Results: NG25 significantly suppressed the tumor progression in immunocompetent Balb/c mice, while concurrently increasing the spleen and thymus indices and promoting the proliferation of T and B lymphocytes. In tumor microenvironment, NG25 treatment could promote CD8+ T cell infiltration and increase the proportion of CD3+CD8+ T cell subsets. Mechanistic studies revealed that NG25 downregulates PD-L1 expression on both *KRAS*-mutant tumor cells and T cells through inhibiting TAK1/NF-κB axis. However, this regulatory effect was absent in *KRAS* wild-type tumor cells.

Conclusion: NG25 blocks the NF-κB signaling pathway by targeting TAK1, remodels the immunosuppressive microenvironment of *KRAS*-mutated colorectal cancer, reduces PD-1 expression and enhances the anti-tumor effect of CD8+ T cells. This study provides a theoretical basis for TAK1-targeted therapy and offers a new strategy for immunotherapy of *KRAS*-mutated colorectal cancer.

Keywords: NG25, tumor immunosuppression, *KRAS* mutation, colorectal cancer

Introduction

Colorectal cancer (CRC) is the third most common malignancy worldwide, with *KRAS* mutations detected in approximately 40% of cases.[1,2] These mutations are associated with poor prognosis and resistance to conventional chemotherapy and epidermal growth factor receptor (EGFR)–targeted therapies.[3] Although immune checkpoint inhibitors (ICIs) have shown promising efficacy in microsatellite instability–high (MSI-H) CRC and non–small cell lung cancer (NSCLC), their clinical benefit remains limited in *KRAS*-mutant tumors. This immune resistance is primarily driven by two mechanisms: *KRAS* mediates the secretion of cytokines such as IL-8 and CCL2, thereby recruiting myeloid-derived suppressor cells (MDSCs) and regulatory T cells (Tregs);[4] concurrently, *KRAS* induces upregulation of PD-L1 expression through the ERK and tristetraprolin (TTP) pathways, leading to impaired T-cell activation and the formation of an immunosuppressive tumor microenvironment (TME).[5] Therefore, identifying effective therapeutic strategies for *KRAS*-mutant CRC remains a pressing challenge.

Transforming growth factor-β–activated kinase 1 (TAK1, also known as MAP3K7) is a key upstream mediator that integrates inflammatory and stress signals into downstream NF-κB and MAPK cascades. Upon stimulation by cytokines

https://doi.org/10.2147/OTT.S540070
Received: 13 May 2025
Accepted: 4 December 2025
Published: 8 January 2026

such as TNF-α, IL-1β, or TGF-β, TAK1 associates with TAK1-binding proteins (TAB1/TAB2/TAB3) and recruits TRAF2 or TRAF6, which catalyze Lys63-linked polyubiquitination at TAK1 Lys158 to promote its activation.[6] Activated TAK1 phosphorylates the IKK complex, leading to IκBα degradation and NF-κB nuclear translocation, thereby inducing transcription of genes involved in inflammation, cell survival, and immune regulation.[7] Aberrant activation of the TAK1–NF-κB axis contributes to chronic inflammation, tumor progression, and immune evasion in multiple malignancies, including CRC.[8–12] These mechanisms provide a strong rationale for targeting TAK1 to suppress tumor growth and remodel the immunosuppressive TME.[12,13]

NG25 is a selective, ATP-competitive TAK1 inhibitor that effectively suppresses its kinase activity.[14] It has demonstrated therapeutic potential in inflammatory disorders and various cancers. In breast cancer, NG25 enhances doxorubicin-induced apoptosis by inhibiting TAK1;[14,15] in CRC, it suppresses tumor proliferation and induces caspase-dependent apoptosis in both cell culture and mouse models.[16] However, the role of NG25 in regulating tumor immunity, particularly within the *KRAS*-mutant CRC microenvironment, remains unclear.

This study aims to elucidate how NG25 modulates the TAK1–NF-κB–PD-L1 signaling axis and reshapes the immunosuppressive TME in *KRAS*-mutant CRC, thereby advancing our understanding of TAK1-targeted immunoregulation and providing a potential therapeutic approach for *KRAS*-driven malignancies.

Materials and Methods

Chemicals and Reagents

NG25 (Cat. No. SML1332) and 5-FU (Cat. No. F6627) were purchased from Sigma-Aldrich (St. Louis, MO, USA). Red Blood Cell Lysis Buffer (Cat. No. C3702) was obtained from Beyotime (Shanghai, China). MidiMACS™ Starting Kits (Cat. No. 130–042-301), LS Columns (Cat. No. 130–041-306), and the Pan T Cell Isolation Kit II (Cat. No. 130–095-130) were acquired from Miltenyi Biotec (Bergisch Gladbach, Germany). The following antibodies were used in this study: IκBα (Cat. No. 4814) and p-IκBα (Cat. No. 2859) from Cell Signaling Technology (CST, Danvers, MA, USA); TAK1 (Cat. No. sc-166562) and p-TAK1 (Cat. No. sc-4531) from Santa Cruz Biotechnology (Dallas, TX, USA); PD-L1 (Cat. No. PA5-20343) from Thermo Fisher Scientific (Waltham, MA, USA); β-actin (Cat. No. A2228) from Sigma-Aldrich (St. Louis, MO, USA); CD3 (Cat. No. 46–0032-80), PD-L1 (Cat. No. 12–5982-81), and CD4 (Cat. No. 553046) from eBioscience (San Diego, CA, USA); CD8α (Cat. No. 553046 and 553041) from BD Biosciences (San Jose, CA, USA); PD-1 (Cat. No. 562671) from BD Pharmingen™ (San Jose, CA, USA) and CD8α (Cat. No. ab217344) from Abcam (Cambridge, UK). HRP-conjugated goat anti-rabbit IgG (Cat. No. 35561) was obtained from Thermo Fisher Scientific (Waltham, MA, USA), and HRP-conjugated goat anti-mouse IgG (Cat. No. ab150113) was acquired from Abcam (Cambridge, UK). DyLight 594-conjugated goat anti-rabbit IgG (Cat. No. 35561) and Alexa Fluor 488-conjugated goat anti-mouse IgG (Cat. No. A11001) were also purchased from Thermo Fisher Scientific (Waltham, MA, USA).

Cell Line and Cell Culture

The $HCT116^{KRASG13D}$, $HCT116^{KRASWT}$ CRC cell lines were kindly provided by Harvard Medical School. The murine colorectal cancer cell line CT26 was obtained from the Kunming Cell Bank (KCB, Kunming, China). All cell lines were maintained in Dulbecco's Modified Eagle Medium (DMEM, high glucose; Thermo Scientific, USA) containing 5% fetal bovine serum (FBS; Gibco, USA), along with 100 U/mL penicillin and 100 μg/mL streptomycin (Thermo Scientific, USA), under standard conditions of 37°C and 5% CO_2 in a humidified atmosphere.

Orthotopic Mouse Model and Treatment

Eight male Balb/c nude mice (6–8 weeks, 22–24 g) and eight male Balb/c mice were acclimated for 7 days in SPF conditions (12 h light/dark, 20 ± 2 °C, 50–60% humidity). Mice were anesthetized with isoflurane (3–5% for induction, 1–2% for maintenance), and $CT26^{KRASG12D}$ cells (2.5×10^6/mouse) were injected into the mesenteric triangle of the cecum.

One-week post-implantation, mice were randomly assigned by immune status: nude mice—control (n = 4, saline 0.3 mL/day) or NG25 (n = 4, 30 μM/kg/day); Balb/c mice—control (n = 4, saline 0.3 mL/day) or NG25 (n = 4, 30 μM/kg/day), all intraperitoneally.

After 7 days of treatment, body weight was recorded, and tumors were collected, photographed, measured, and weighed. Tumor volume (V) was calculated using the following formula:

$$V = \frac{(length \times width \times height \times \pi)}{6}$$

The spleen index and thymus index were calculated as follows:

$$Spleen\ index = \frac{spleen\ weight}{body\ weight}\ Thymus\ index = \frac{thymus\ weight}{body\ weight}$$

Magnetic Separation of T Lymphocytes

The spleens from Balb/c mice were gently ground to obtain a single-cell suspension, followed by centrifugation to remove the supernatant. Red blood cells were lysed by adding 3–5 times the volume of red blood cell lysis buffer and gently pipetting for 1–2 minutes. The mixture was centrifuged at 4°C (500 × g, 5 minutes), and the red supernatant was discarded. The remaining cell pellet was resuspended in PBS and centrifuged again (500 × g, 3 minutes). The supernatant was discarded. T lymphocytes were isolated using the Pan T Cell Isolation Kit II, mouse (Cat. No. 130–095-130; Miltenyi Biotec), following the manufacturer's instructions. The cell suspension was adjusted to a concentration of 1×10^7 cells/40 μL. For each 1×10^7 cells, 10 μL of Biotin-Antibody Cocktail was added, mixed gently, and incubated at 4 °C for 5 minutes. Subsequently, 10 μL of buffer and 20 μL of Anti-Biotin MicroBeads were added and mixed thoroughly. The LS column was placed on a magnetic separator and pre-equilibrated with 2 mL of buffer. The labeled cell suspension was then applied to the column, and unbound cells were collected as the flow-through. The column was washed with 3 mL of buffer, and the wash fractions were combined with the initial flow-through to obtain the purified splenic T lymphocyte population.

Lymphocyte Co-Culture and Flow Cytometric Analysis of T-Cell Surface Antigen Expression

The magnetically sorted T lymphocytes were resuspended and counted. A total of 5×10^6 T lymphocytes were co-cultured with 5×10^5 CT26 cells in a six-well plate for 24 h. NG25 (5 μM) was added to the co-culture system for 48 h. Cells were then collected by centrifugation and stained with antibodies against T lymphocyte surface markers according to the manufacturer's instructions: anti-CD3 (Cat. No. 46-0032-80; eBioscience), anti-CD4 (Cat. No. 553046; eBioscience), anti-CD8α (Cat. No. ab217344; Abcam), and anti-PD-1 (Cat. No. 562671; BD Pharmingen™). Flow cytometry was performed using the PerCP channel for CD3, FITC for CD4, and PE for CD8 and PD-L1. Data acquisition and analysis were conducted with CXP software (Beckman Coulter, USA) to assess T lymphocyte differentiation and PD-L1 expression.

Lymphocyte Expansion Assay Was Used to Detect Immune Function

Splenic lymphocytes were isolated and resuspended at a density of 5×10^6 cells/mL. A total of 100 μL of the cell suspension was seeded into each well of a 96-well plate. Cells were stimulated with phytohemagglutinin (PHA), lipopolysaccharide (LPS), or a combination of both, and cultured for 72 hours. Subsequently, 20 μL MTT reagent (5 mg/mL) was added into each well and cells were further incubated at 37°C for 4 hours. Following removing the supernatant, the formazan precipitate was solubilized using 150 μL of DMSO. The optical density (OD) was measured at 540 nm. The calculation of stimulation index (SI) employed the equation presented below:

$$SI = \frac{(OD\ stimulated\ group - OD\ background)}{(OD\ control\ group - OD\ background)}$$

 https://doi.org/10.2147/OTT.S540070

Western Blot Analysis of Protein Expression Levels

$HCT116^{KRASG13D}$ and $HCT116^{KRASWT}$ cell lines were treated with varying concentrations of NG25 for 48 hours. Adherent cells were collected and subjected to centrifugation to obtain pellets. Total protein was isolated using RIPA lysis buffer (Beyotime Biotechnology, China), followed by concentration determination through Bradford methodology (Bio-Rad, USA). Equal quantities of protein (20 μg per sample) were separated by SDS-PAGE and transferred onto PVDF (Millipore, USA) membranes by electroblotting. The membranes were then blocked in TBST containing 5% non-fat milk for 1 hour at room temperature. An overnight incubation with primary antibodies was performed at 4°C. After thorough washing, HRP-labeled secondary antibodies (Cell Signaling Technology, USA) were added and incubated for 1 hour at room temperature. Protein signals were detected with the ECL Select™ Western Blotting Detection Reagent (RPN2235, GE Healthcare, UK) and visualized using the ImageQuant™ LAS 4000 imaging system (GE Healthcare). Intensities analysis of the bands was performed using ImageJ software (NIH, USA), with β-actin employed as an internal loading control.

RT-PCR Analysis of Gene Expression

$HCT116^{KRASG13D}$ and $HCT116^{KRASWT}$ cells were treated with NG25 for 48 hours. The supernatants and adherent cells were both collected for subsequent analysis. Total RNA was isolated using TRIzol reagent (Thermo Scientific, USA) in accordance with the manufacturer's instructions. 1 μg RNA was used for complementary DNA (cDNA) synthesis with the RevertAid First Strand cDNA Synthesis Kit (#1622, Thermo Scientific). qPCR analysis was carried out on the 7500 Real-Time PCR System (Applied Biosystems) using the FastStart Universal SYBR Green Master (ROX) mix (Cat. No. 19317900, Roche). The primers used for TAK1 amplification: forward 5′-GATGCGGTACTTTCCAGGAG-3′, reverse 5′-CATGAATGAGCCTGTACTGGTG-3′. Relative gene expression levels were calculated using the $2^{-\Delta\Delta Ct}$ method, with GAPDH serving as the internal control for normalization.

Immunohistochemical (IHC) Staining

Colonic cancer tissue from mice, embedded in paraffin, were blocked with 5% goat serum at 37°C for 1 hour and incubated overnight at 4°C with primary antibodies against CD3 and CD8. The next day, sections were rewarmed at 37°C for 45 minutes. Subsequently, secondary antibodies were applied and incubated at 37°C for 1 hour. After washing, sections were incubated with DAB substrate in the dark until visible brown staining developed, followed by counter-staining with hematoxylin for 5 minutes. Sections were then differentiated in 1% hydrochloric acid-alcohol, rinsed under running water, and blued in warm tap water (55°C) for 30 minutes. Finally, tissues were dehydrated through an ethanol series. For quantitative analysis, five randomly selected high-power fields (×400 magnification) per sample were imaged, and 100 cells per field were scored based on staining intensity and the percentage of positive cells, using ImageJ software to analyze (NIH, USA).

Statistical Analysis

Statistical analyses were performed using SPSS v24.0 (IBM, USA), and graphs were generated with GraphPad Prism. Data are presented as mean ± SD. For normally distributed data, two-group comparisons were conducted using Student's *t*-test, and multiple-group comparisons were performed using one-way ANOVA. Non-normally distributed data were analyzed with nonparametric tests (Mann–Whitney *U*-test for two groups, Kruskal–Wallis test for multiple groups). A p-value < 0.05 was considered statistically significant.

Results

The Anti-Tumor Efficacy of NG25 is Associated with Host Immune Competence

To assess whether the host immune function contributes to the anti-tumor efficacy of NG25, we established orthotopic colorectal cancer models using both immunodeficient Balb/c nude mice and immunocompetent Balb/c mice. Following intraperitoneal injection of $CT26^{KRASG12D}$ cells and 7 days of treatment, NG25 exhibited a degree of tumor inhibition in the immunodeficient Balb/c nude mouse model (Figure 1A and B). However, a marked difference in therapeutic efficacy was observed between the two groups. In immunocompetent group, NG25 treatment resulted in an approximately 80%

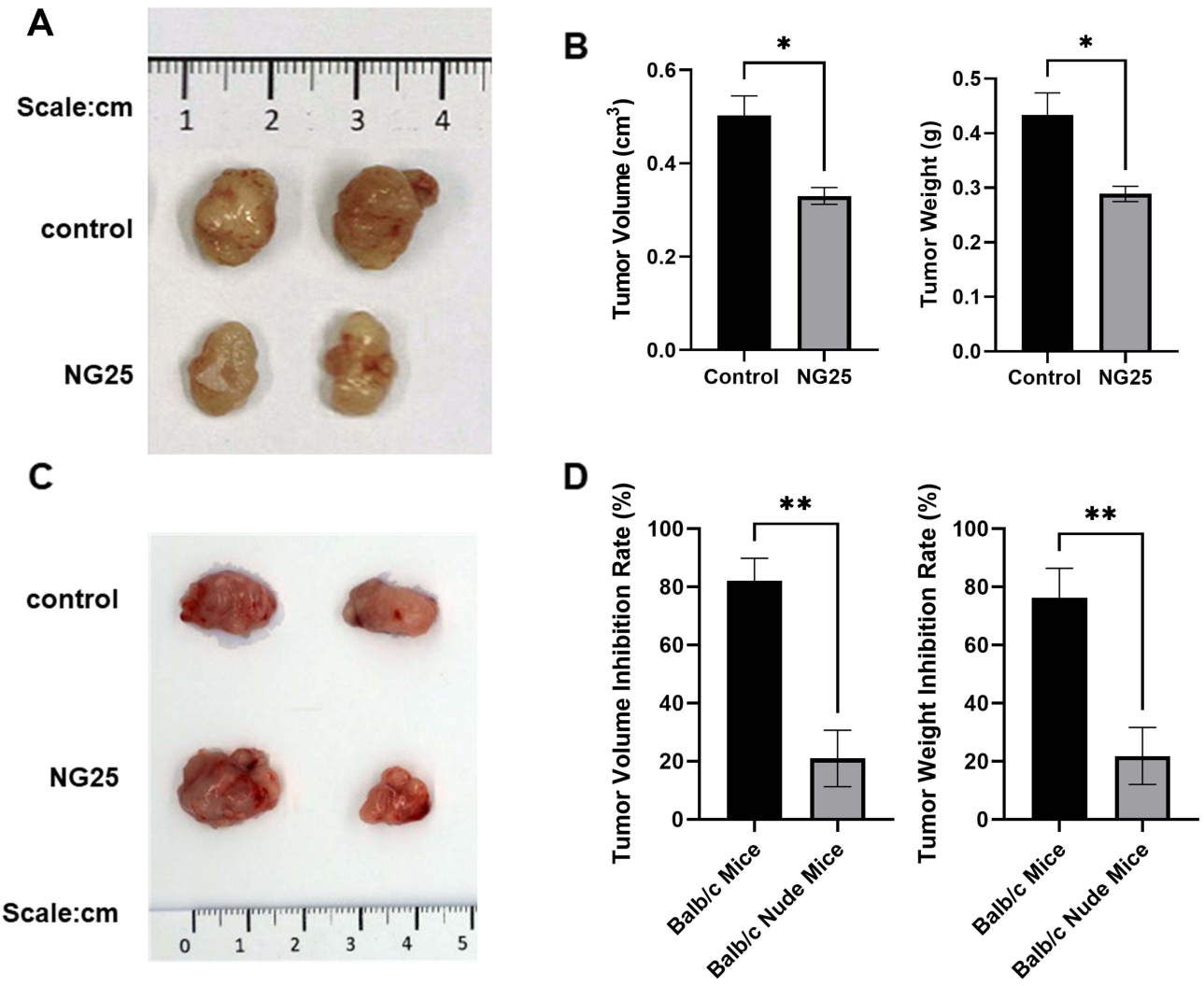

Figure 1 NG25 exhibits stronger anti-tumor activity in immunocompetent orthotopic CRC models. (**A**) Representative images of orthotopically implanted colorectal tumors isolated from immunodeficient Balb/c nude mice after 7 days of intraperitoneal treatment with normal saline (N.S.) or NG25 (30 μM/kg/day, administered once daily). n = 4. (**B**) Tumor size and weight were recorded at the time of tissue collection. (**C**) Representative images of orthotopic CRC tumors isolated from immunocompetent Balb/c mice after 7 days of intraperitoneal administration of N.S or NG25 (30 μM/kg/day, once daily). n = 4. (**D**) NG25 demonstrated a stronger suppressive effect on tumor growth in immunocompetent mice. Tumor growth inhibition rate (%) = [(control group mean - treatment group mean)/control group mean] × 100. Data are presented as mean ± SD. *p < 0.05, **p < 0.01.

reduction in tumor volume compared to the normal saline (N.S.) control group, whereas in nude mice, the inhibition rate was about 20% (Figure 1C and D). These results suggest that the anti-tumor effects of NG25 are, at least in part, dependent on the presence of a functional immune system.

NG25 Enhances Multilevel Immune Function in Mice

To further investigate the effects of NG25 on host immune competence, we evaluated the thymus index and spleen indices in orthotopic CRC mouse models, which serve as indicators of the systemic immune status. Compared with N. S. control group, NG25 treatment significantly increased the spleen index and thymus indices, suggesting enhanced function of immune organs. (Figure 2A and B) NG25 also promoted immune activity: lymphocyte proliferation assays demonstrated that NG25 treatment enhanced the in vitro proliferative capacity of both T and B cells (Figure 2C–E). In contrast, treatment with the conventional chemotherapeutic agent 5-fluorouracil (5-FU) inhibited lymphocyte proliferation, consistent with previous reports of 5-FU-induced immunosuppression observed in clinical settings[17] (Figure 2A–E).

https://doi.org/10.2147/OTT.S540070

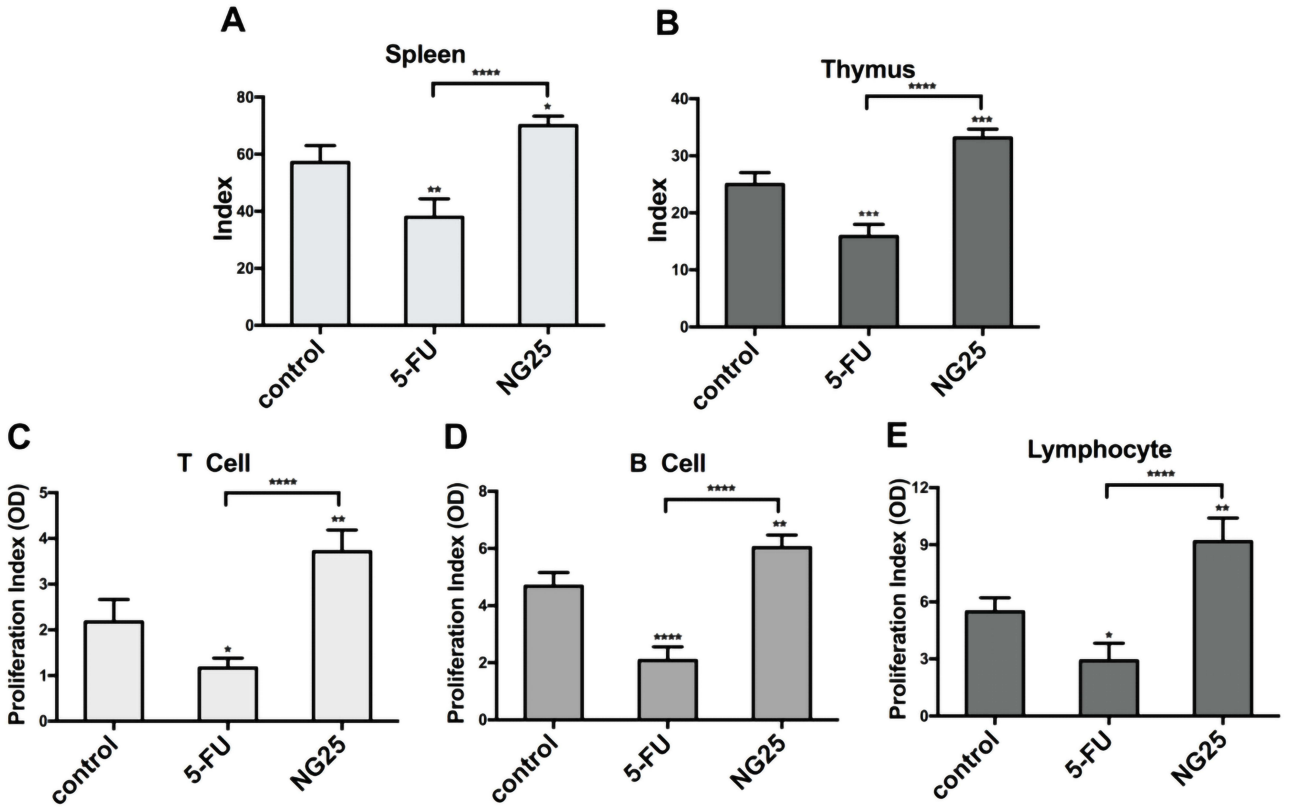

Figure 2 NG25 enhances the immune function of both organ and cellular levels. (**A**) Mouse spleens from different treatment groups were surgically isolated, and the spleen index was calculated after measured spleen weight. (**B**) The thymus index was obtained by the same method. Compared with the control group, NG25 treatment improved the spleen and thymus index, while 5-FU reduced them. (**C**) Magnetic bead separation was used to isolate splenic lymphocytes. Evaluating the T lymphocyte proliferation index after phytohemagglutinin (PHA) treatment. (**D**) Evaluating the B lymphocyte proliferation index after Lipopolysaccharide (LPS) treatment. (**E**) Total lymphocyte proliferation was evaluated by co-stimulating treatment with PHA and LPS. NG25 treatment significantly upregulated the proliferation index of T lymphocyte, B lymphocyte, and total lymphocytes. However, 5-FU still exhibited the opposite effect. Data are presented as mean ± SD (n = 4). *p < 0.05, **p < 0.01, ***p < 0.001, ****p < 0.0001.

NG25 Promotes the Formation of an Anti-Tumor Tumor Microenvironment

Immunohistochemical (IHC) analysis revealed that NG25 treatment markedly increased CD3+CD8+ T cell infiltration in orthotopic colorectal tumors, suggesting that NG25 enhanced cytotoxic T lymphocyte (CTL) recruitment. (Figure 3A) To further investigate the effect of NG25 on T cell function, we established an in vitro co-culture model of CT26 tumor cells and CD3+ lymphocytes. After 48 hours of NG25 exposure, surface marker expression on T cells was analyzed by flow cytometry. (Figure 3B–E and Figure S4-5) The results showed significant alterations in T cell differentiation. The proportion of $CD3^+CD8^+$ T cells increased from 6% to 14%, while the proportion of $CD3^+CD4^+$ T cells decreased from42.1% to 22.3%. (Figure 3F) These findings suggest that NG25 promotes anti-tumor immunity through dual mechanisms—enhancing CTL recruitment and increasing the proportion of CTLs within the tumor microenvironment.

NG25 Regulates PD-L1 Expression Through a KRAS Mutation–Dependent Mechanism

PD-L1 plays a critical immunosuppressive role within the tumor microenvironment (TME) by engaging PD-1 receptors on the surface of T cells, thereby inhibiting anti-tumor immune responses.[18] To examine whether NG25 modulates PD-L1 expression, CRC cells were treated with NG25 and both mRNA and protein levels were assessed. Treatment of $HCT116^{KRASG13D}$ cells with NG25 (2.5 μM or 5 μM) for 48 h led to a marked downregulation of PD-L1 protein, particularly at 5 μM. In contrast, PD-L1 protein levels in $HCT116^{KRASWT}$ cells did not show a comparable decrease (Figure 4A and Figure S1). Consistently, PD-L1 mRNA analysis revealed significant transcriptional downregulation only in $HCT116^{KRASG13D}$ cells upon 5 μM NG25 treatment, whereas $HCT116^{KRASWT}$ cells remained unaffected under the

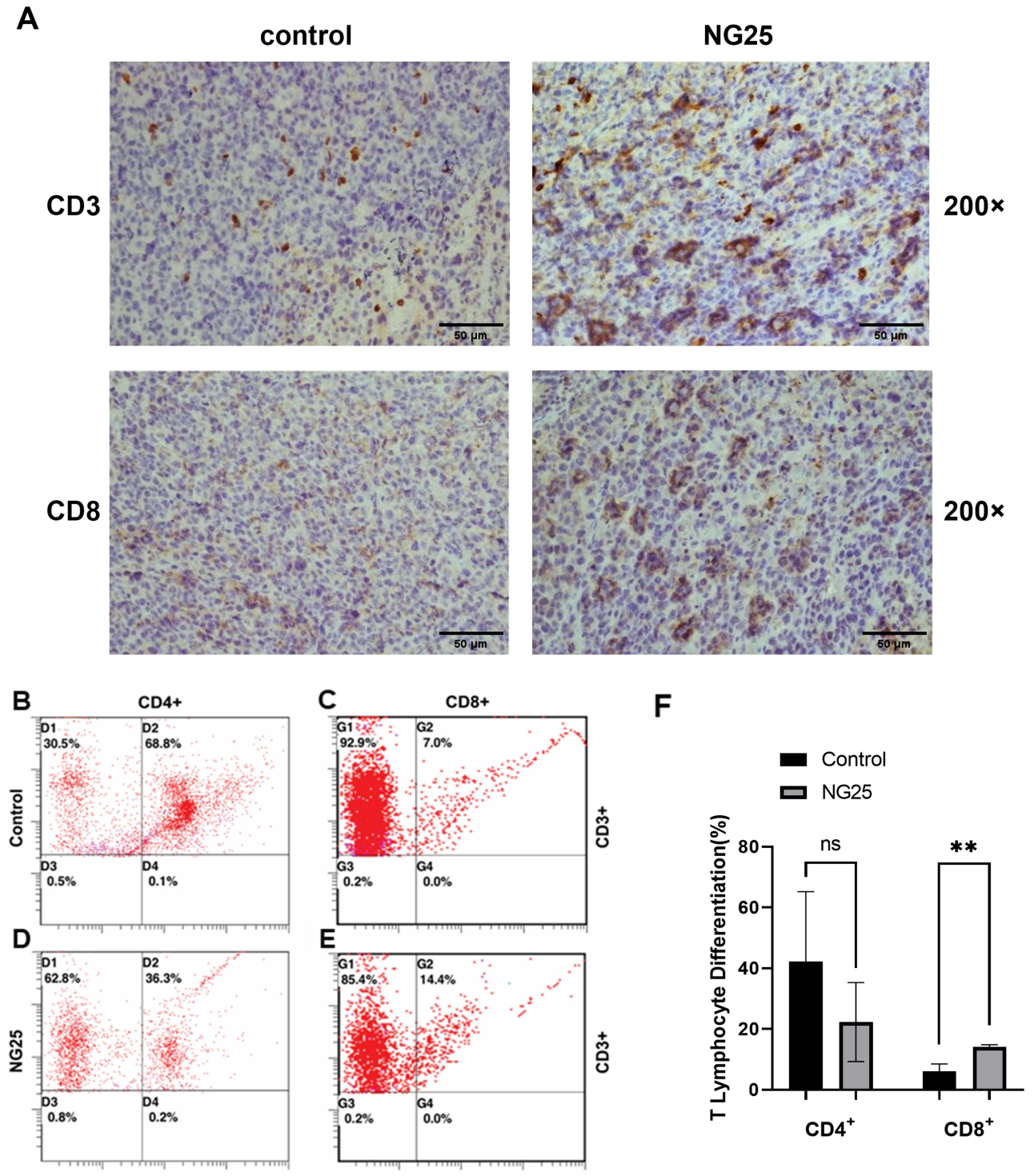

Figure 3 NG25 promotes $CD8^+$T cell infiltration and differentiation in tumor tissues. (**A**) Immunohistochemical (IHC) staining was used to detect CD3 and CD8 expression in orthotopic colorectal cancer tissue of mice, which has been treated with NG25 and N.S. The infiltration of $CD3^+CD8^+$ cells was significantly higher in NG25 treatment group. (magnification: 200×) (**B**–**E**) The co-culture system of Balb/c mouse spleen $CD3^+$ cells and $CT26^{KRASG12D}$ cells was treated with NG25 for 48h. $CD3^+$ cells were collected for $CD8^+$, $CD4^+$ staining on their surface, and $CD8^+$, $CD4^+$ expression was detected by flow cytometry. (**F**) NG25 significantly promotes the CD3+ T cells differentiating into CD3+CD8+ T cells. The experiment was performed in triplicate, and a representative image is shown. Data are presented as mean ± SD (n = 3), **p < 0.01.

https://doi.org/10.2147/OTT.S540070

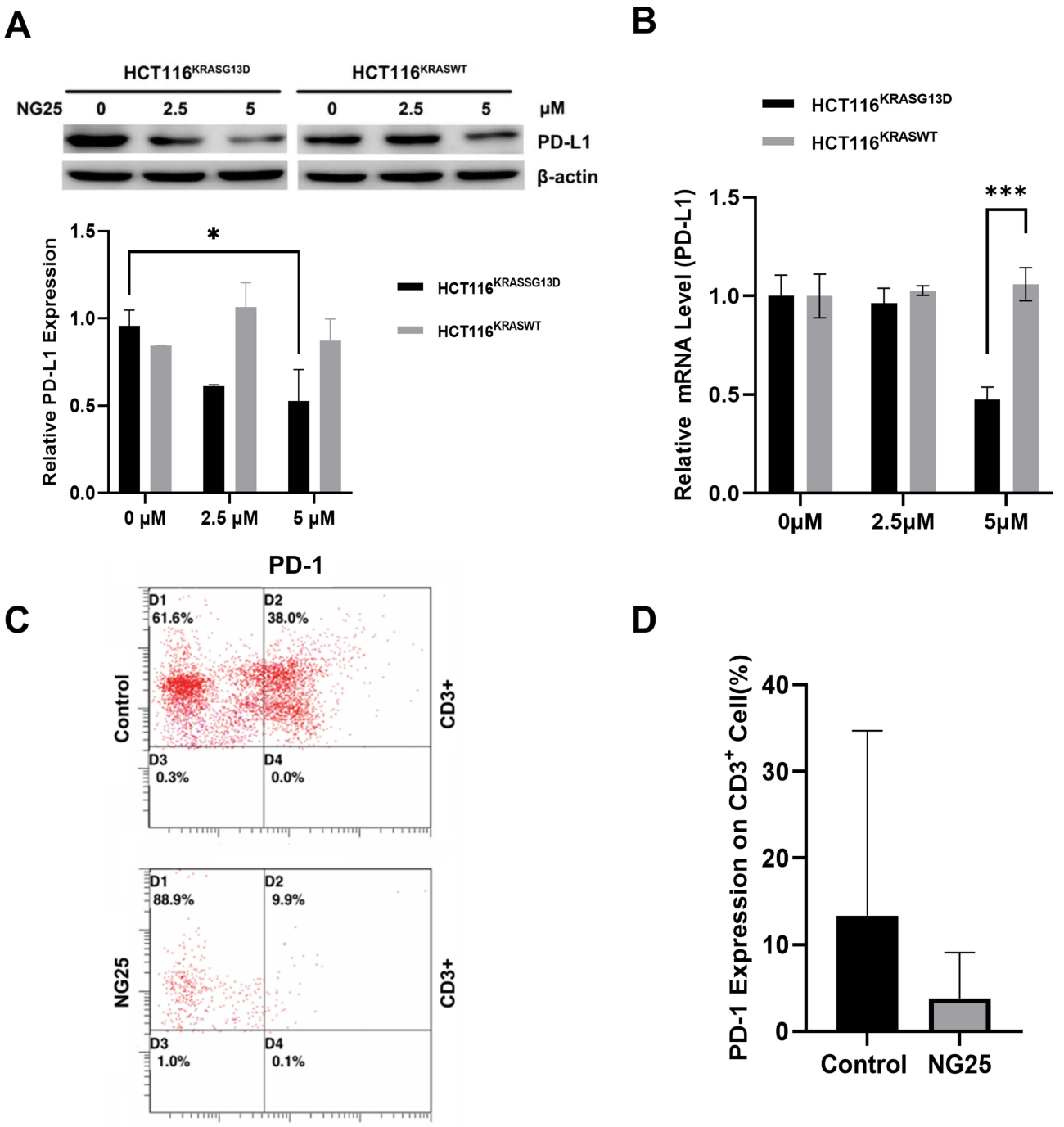

Figure 4 NG25 reduces PD-L1 expression level in *KRAS*-mutant CRC. (**A**) PDL1's protein level in HCT116^{KRASG13D} and HCT116^{KRASWT} following 48-hour exposure to NG25 at 2.5 μM and 5 μM. (**B**) PD-L1 mRNA levels were assessed by RT-PCR. NG25 significantly inhibited PD-L1 expression in HCT116^{KRASG13D} cells at the concentration of 5 μM. (**C**) PD-1 expression on the surface of CD3+ T cells from the lymphocyte and tumor cell co-culture system with NG25 treated, which was measured by flow cytometry. (**D**) NG25 suppressed PD-1 expression on CD3+ T cells. *$p < 0.05$, ***$p < 0.001$.

same conditions (Figure 4B). These results indicate that NG25-mediated PD-L1 inhibition is specifically dependent on *KRAS* mutation status.

Importantly, NG25 also affected immune cells. In a co-culture of CT26 cells with CD3+ T cells isolated from Balb/c mouse spleens, 48 h of NG25 treatment reduced the proportion of PD-1–positive CD3+ T cells from 13.33% to 3.8% (Figure 4C, D and Figure S6). Together, these findings suggest that NG25 may remodel the immunosuppressive TME by downregulating PD-1 expression in T cells and PD-L1 expression in tumor cells through a *KRAS* mutation–dependent mechanism.

https://doi.org/10.2147/OTT.S540070

NG25 Suppresses PD-L1 and PD-1 Expression Through the TAK1/NF-κB Signaling Axis

To clarify the mechanism by which NG25 downregulates PD-L1, we focus on the classical downstream effector pathway NF-κB of TAK1. NF-κB activation is widely implicated in promoting PD-L1 expression and establishing immunosuppressive tumor microenvironments.[19,20] In this pathway, IκBα, as a key inhibitory protein, exerts regulatory effects by anchoring NF-κB in the cytoplasm. When IκBα is phosphorylated and degraded by IKK, NF-κB can enter the nucleus to initiate the transcription process.

Based on the report that NG25 can target TAK1 to inhibit the NF-κB pathway in *KRAS*-mutated colorectal cancer,[16] we speculate that NG25 may regulate PD-L1 through this pathway. The results showed that the NF-κB inhibitor PDTC treated HCT116^{KRASG13D}. The results showed that treatment of HCT116^{KRASG13D} cells with the NF-κB inhibitor PDTC reduced PD-L1 expression (Figure 5A and Figure S2); Similarly, NG25 treatment markedly decreased PD-L1 expression

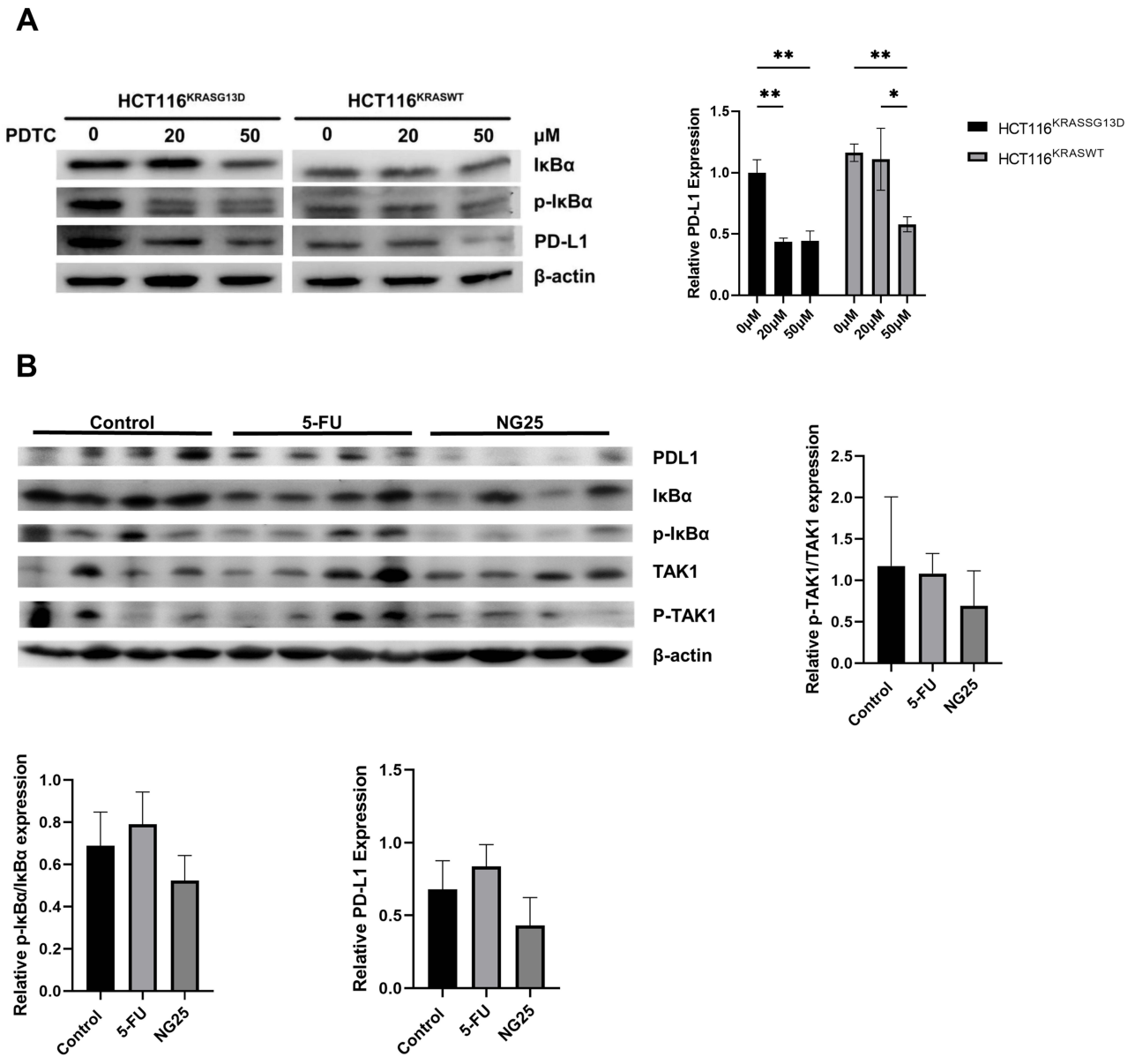

Figure 5 NG25 inhibits PD-L1 expression by blocking the NF-κB pathway. (**A**) Western blot analysis of the activation level of NF-κB and the expression of PD-L1 in HCT116^{KRASG13D}, HCT116^{KRASWT} which were treated by NF-κB inhibitor PDTC (20 μM or 50 μM) for 24 hours. The expression of PD-L1 was decreased while the activation of NF-κB was inhibited. (**B**) Western blot analysis of the expression of PD-L1, and phosphorylation level of TAK1, IκBα. NG25 treatment inhibited NF-κB activation and PD-L1 expression in tumor tissues. *p < 0.05, **p < 0.01.

https://doi.org/10.2147/OTT.S540070

in *KRAS*-mutant colorectal cancer cells (Figure 4A and B). Moreover, in tumor tissues from orthotopic colorectal cancer-bearing mice treated with NG25, PD-L1 expression was suppressed, accompanied by decreased IκBα phosphorylation, a key marker of NF-κB activation (Figure 5B and Figure S3). These findings demonstrate that NG25 downregulates PD-L1 expression through the TAK1/NF-κB signaling axis, thereby reducing T cell inhibition and promote anti-tumor immune responses.

Discussion

The progression of colorectal cancer (CRC) involves a complex interplay between oncogenic mutations and the tumor immune microenvironment.[8,20] Among these, *KRAS*-mutant CRC exhibits particularly poor outcomes due to limited targeted therapies and immune resistance.[21,22] Transforming growth factor-β-activated kinase 1 (TAK1), a central hub linking NF-κB and MAPK signaling, regulates tumor cell survival, inflammation, and immune modulation.[8] Aberrant TAK1 activation has been implicated in multiple malignancies, including CRC, and is associated with poor prognosis, making TAK1 a promising therapeutic target.[8,13,20,23]

In this study, we demonstrate that the TAK1 inhibitor NG25 suppresses tumor growth and enhances anti-tumor immunity in *KRAS*-mutant CRC, and this therapeutic effect is related to the body's immunity.[11,16] NG25 treatment remodeled the tumor microenvironment by promoting CD8+ T cell infiltration and downregulating PD-L1 expression in tumor cells and PD-1 expression in T cells through inhibition of the TAK1/NF-κB signaling axis.[23] These findings reveal that NG25 exerts dual anti-tumor and immunomodulatory effects, providing a rationale for TAK1-targeted therapy in immune-refractory CRC.

Our results suggest that the enhanced CD8+ T cell infiltration and proliferation reflect a more immune-activated tumor microenvironment. Previous studies support that NF-κB inhibition—via TAK1 blockade or Sirt1 activation—reduces proinflammatory cytokines such as IL-1β and IL-6,[24] indicating that NG25 may also reshape cytokine networks to restore immune balance. Moreover, PD-L1 downregulation by NG25 is consistent with the role of NF-κB in PD-L1 transcriptional control,[25–27] further supporting the mechanistic link between TAK1 inhibition and immune reactivation.

Despite these promising observations, several limitations should be acknowledged. The current study does not directly assess the cytotoxic functionality of CD8+ T cells; functional assays such as intracellular IFN-γ or Granzyme B staining are required for confirmation. The interpretation of spleen and thymus indices also warrants caution, as splenic enlargement has been associated with poor prognosis in clinical settings.[28–30] Additionally, whether NG25 modulates antigen presentation (eg, MHC-I expression) remains to be determined.[9,31,32] Finally, the long-term efficacy and safety of NG25 require further validation in extended preclinical and translational studies.

Moving forward, we aim to elucidate the detailed mechanisms by which NG25 reshapes the CRC immune microenvironment—particularly its regulation of immune-related transcriptional networks, cytokine signaling, and tumor antigen presentation. Integration of transcriptomic and bioinformatic analyses, alongside comprehensive pharmacological evaluation, will deepen understanding of NG25's immunomodulatory potential and guide rational combination strategies for *KRAS*-mutant CRC therapy.

Conclusion

In summary, regarding anti-tumor efficacy and immune microenvironment remodeling, we demonstrate that NG25 treatment significantly inhibits the proliferation of *KRAS*-mutant colorectal cancer cells and tumor growth, and reshapes the immunosuppressive tumor microenvironment by modulating PD-L1 expression on tumor cells and PD-1 expression on T cells, enhancing CD8+ T cell differentiation and infiltration. We propose that the anti-tumor activity of NG25 is mediated through the TAK1-NF-κB potentially immunoregulatory axis. These findings provide a theoretical foundation for the development of TAK1 inhibitor-based immunotherapies and offer a promising new therapeutic strategy for *KRAS*-mutant CRC.

Abbreviations

CRC, colorectal cancer; TAK1, transforming growth factor-β-activated kinase 1; MDSCs, myeloid-derived suppressor cells; NSCLC, non-small cell lung cancer; ICIs, immune checkpoint inhibitors; Tregs, regulatory T cells; TTP, tristetraprolin; TME, tumor microenvironment; IL-1β, interleukin-1β; PDAC, pancreatic ductal adenocarcinoma; GBM,

glioblastoma; IHC, immunohistochemistry; WT, wild-type; LPS, lipopolysaccharide; PHA, phytohemagglutinin; OD, optical density; SI, stimulation index.

Data Sharing Statement

The original contributions presented in this study are included in the article. Further inquiries can be directed to the first author or the corresponding author Yufang Wang (wangyufang@scu.edu.cn).

Ethics Approval and Informed Consent

All animal experiments were approved by the Institutional Animal Care and Use Committee (IACUC) of the Laboratory Animal Center, Sichuan University and conducted in accordance with institutional and national guidelines. And the use of $HCT116^{KRASG13D}$ and $HCT116^{KRASWT}$ cells was approved by Medical Ethics Committee of Sichuan University (KS202548).

Funding

This work was funded by grants from the National Natural Science Foundation of China (Grant Nos. 82173104, 81871233, and 82230064).

Disclosure

The authors report no conflicts of interest in this work.

References

1. Zhu G, Pei L, Xia H, Tang Q, Bi F. Role of oncogenic KRAS in the prognosis, diagnosis and treatment of colorectal cancer. *Mol Cancer*. 2021;20(1):143. doi:10.1186/s12943-021-01441-4
2. Eng C, Yoshino T, Ruíz-García E, et al. Colorectal cancer. *Lancet*. 2024;404(10449):294–310. doi:10.1016/S0140-6736(24)00360-X
3. Zhu C, Guan X, Zhang X, et al. Targeting KRAS mutant cancers: from druggable therapy to drug resistance. *Mol Cancer*. 2022;21(1):159. doi:10.1186/s12943-022-01629-2
4. Huang L, Guo Z, Wang F, Fu L. KRAS mutation: from undruggable to druggable in cancer. *Signal Transduction Targeted Ther*. 2021;6(1):386. doi:10.1038/s41392-021-00780-4
5. Coelho MA, de Carné Trécesson S, Rana S, et al. Oncogenic RAS signaling promotes tumor immunoresistance by stabilizing PD-L1 mRNA. *Immunity*. 2017;47(6):1083–1099.e1086. doi:10.1016/j.immuni.2017.11.016
6. Collie GW, Clark MA, Keefe AD, et al. Screening ultra-large encoded compound libraries leads to novel protein–ligand interactions and high selectivity. *J Med Chem*. 2024;67(2):864–884. doi:10.1021/acs.jmedchem.3c01861
7. Fan G, Lu J, Zha J, et al. TAK1 in vascular signaling: "friend or foe"? *J Inflamm Res*. 2024;17:3031–3041. doi:10.2147/JIR.S458948
8. Mukhopadhyay H, Lee NY. Multifaceted roles of TAK1 signaling in cancer. *Oncogene*. 2020;39(7):1402–1413. doi:10.1038/s41388-019-1088-8
9. Sheng N, Shindo K, Ohuchida K, et al. TAK1 promotes an immunosuppressive tumor microenvironment through cancer-associated fibroblast phenotypic conversion in pancreatic ductal adenocarcinoma. *Clin Cancer Res*. 2024;30(22):5138–5153. doi:10.1158/1078-0432.CCR-24-1004
10. Damhofer H, Tatar T, Southgate B, et al. TAK1 inhibition leads to RIPK1-dependent apoptosis in immune-activated cancers. *Cell Death Dis*. 2024;15(4):273. doi:10.1038/s41419-024-06654-1
11. Singh A, Sweeney MF, Yu M, et al. TAK1 inhibition promotes apoptosis in KRAS-dependent colon cancers. *Cell*. 2012;148(4):639–650. doi:10.1016/j.cell.2011.12.033
12. Ma P, Jin X, Fan Z, et al. Super-enhancer receives signals from the extracellular matrix to induce PD-L1-mediated immune evasion via integrin/BRAF/TAK1/ERK/ETV4 signaling. *Cancer Biol Med*. 2021;19(5):669–684.
13. Campolo M, Lanza M, Casili G, et al. TAK1 inhibitor enhances the therapeutic treatment for glioblastoma. *Cancers*. 2020;13(1):41.
14. Tan L, Nomanbhoy T, Gurbani D, et al. Discovery of type II inhibitors of TGFβ-activated kinase 1 (TAK1) and mitogen-activated protein kinase kinase kinase kinase 2 (MAP4K2). *J Med Chem*. 2015;58(1):183–196. doi:10.1021/jm500480k
15. Wang Z, Zhang H, Shi M, et al. TAK1 inhibitor NG25 enhances doxorubicin-mediated apoptosis in breast cancer cells. *Sci Rep*. 2016;6:32737. doi:10.1038/srep32737
16. Ma Q, Gu L, Liao S, et al. NG25, a novel inhibitor of TAK1, suppresses KRAS-mutant colorectal cancer growth in vitro and in vivo. *Apoptosis*. 2019;24(1–2):83–94. doi:10.1007/s10495-018-1498-z
17. Wu Y, Deng Z, Wang H, Ma W, Zhou C, Zhang S. Repeated cycles of 5-fluorouracil chemotherapy impaired anti-tumor functions of cytotoxic T cells in a CT26 tumor-bearing mouse model. *BMC Immunol*. 2016;17(1):29. doi:10.1186/s12865-016-0167-7
18. Wu H, Deng M, Xue D, et al. PD-1/PD-L1 inhibitors for early and middle stage microsatellite high-instability and stable colorectal cancer: a review. *Int J Colorectal Dis*. 2024;39(1):83. doi:10.1007/s00384-024-04654-3
19. Rong D, Sun G, Zheng Z, et al. MGP promotes CD8(+) T cell exhaustion by activating the NF-κB pathway leading to liver metastasis of colorectal cancer. *Int J Biol Sci*. 2022;18(6):2345–2361. doi:10.7150/ijbs.70137
20. Shim JH, Xiao C, Paschal AE, et al. TAK1, but not TAB1 or TAB2, plays an essential role in multiple signaling pathways in vivo. *Genes Dev*. 2005;19(22):2668–2681. doi:10.1101/gad.1360605
21. Bteich F, Mohammadi M, Li T, et al. Targeting KRAS in colorectal cancer: a bench to bedside review. *Int J Mol Sci*. 2023;24(15):12030. doi:10.3390/ijms241512030

22. Zhou Y, Kuang Y, Wang C, Yu Y, Pan L, Hu X. Impact of KRAS mutation on the tumor microenvironment in colorectal cancer. *Int J Biol Sci*. 2024;20(5):1947–1964. doi:10.7150/ijbs.88779
23. Galbraith NJ, Quinn JA, Al-Badran SS, et al. TAK1 expression is associated with increased PD-L1 and decreased cancer-specific survival in microsatellite-stable colorectal cancer. *Transl Oncol*. 2024;48:102064. doi:10.1016/j.tranon.2024.102064
24. Li Y, Xi Y, Tao G, et al. Sirtuin 1 activation alleviates primary biliary cholangitis via the blocking of the NF-κB signaling pathway. *Int Immunopharmacol*. 2020;83:106386. doi:10.1016/j.intimp.2020.106386
25. Duan X, Yeerkenbieke G, Huang S, Feng Y. USP32 promotes colorectal carcinoma progression through activating NF-κB signalling pathway. *J Cell Mol Med*. 2025;29(6):e70457. doi:10.1111/jcmm.70457
26. Sun XJ, Zhang JL, Dong BQ, et al. Targeting SLITRK4 restrains proliferation and liver metastasis in colorectal cancer via regulating PI3K/AKT/NFκB pathway and tumor-associated macrophage. *Adv Sci*. 2025;12(1):2400367.
27. McKenzie M, Lian GY, Pennel KAF, Quinn JA, Jamieson NB, Edwards J. NFκB signalling in colorectal cancer: examining the central dogma of IKKα and IKKβ signalling. *Heliyon*. 2024;10(12):e32904. doi:10.1016/j.heliyon.2024.e32904
28. Zhang Y, Fu X, Zhang L, Zhou Q, Wang W. Splenic volume as a predictor of survival in cancer patients treated with immune checkpoint inhibitors. *Front Immunol*. 2025;16:1598484. doi:10.3389/fimmu.2025.1598484
29. Aslan V, Karabörk Kılıç AC, Rustamova Cennet N, et al. Splenic index score as a predictor of outcomes in metastatic non small cell lung cancer patients treated with immune checkpoint inhibitors. *Sci Rep*. 2025;15(1):15781. doi:10.1038/s41598-025-00708-w
30. Zeng Z, Liu Z, Li J, et al. Baseline splenic volume as a biomarker for clinical outcome and circulating lymphocyte count in gastric cancer. *Front Oncol*. 2022;12:1065716. doi:10.3389/fonc.2022.1065716
31. Thiefes A, Wolter S, Mushinski JF, et al. Simultaneous blockade of NFκB, JNK, and p38 MAPK by a kinase-inactive mutant of the protein kinase TAK1 sensitizes cells to apoptosis and affects a distinct spectrum of tumor necrosis target genes. *J Biol Chem*. 2005;280(30):27728–27741. doi:10.1074/jbc.M411657200
32. Schneider AT, Koppe C, Crouchet E, et al. A decision point between transdifferentiation and programmed cell death priming controls KRAS-dependent pancreatic cancer development. *Nat Commun*. 2025;16(1):1765. doi:10.1038/s41467-025-56493-7